Special Feature: Popularizing Fuel Cell Vehicles: Designing and Controlling Electrochemical Reactions in the MEA

Research Report

Oxygen Reduction Reaction Activity Measurement for Fuel Cell Catalysts Using the Rotating Disk Electrode Technique

Kazuma Shinozaki, Yu Morimoto, Jason W. Zack, Svitlana Pylypenko, Ryan M. Richards, Bryan S. Pivovar and Shyam S. Kocha

Report received on Oct. 16, 2018

ABSTRACT Details of the thin-film rotating disk electrode (RDE) technique were studied to propose a standard to obtain accurate and reproducible oxygen reduction reaction (ORR) activities for PEMFC catalysts because the technique is being extensively used for newly developed catalysts, which are normally synthesized only on the mg-scale, but discrepancies in the baseline activity values of reference catalyst materials reported in the literature make it difficult to evaluate the significance of novel catalysts. In this report, appropriate preparation of the RDE apparatus and protocols were determined based on systematic studies. The impact of catalyst film quality was also studied by employing Pt/C catalyst films fabricated using several ink formulations and film-drying techniques. Nafion-free thin uniform catalyst films fabricated in our study exhibited the highest and most reproducible activity for commercial reference Pt/C catalysts due to minimized O_2 diffusion and proton transfer resistances within catalyst film. By applying best practices, the effect of Pt particle size on the ORR activity was re-evaluated. The impact of Nafion ionomer on the ORR activity was also investigated for Pt/C catalysts.

KEYWORDS PEMFC Catalysts, ORR Activity, Rotating Disk Electrode Technique

1. Introduction

Although automotive manufacturers have recently started commercializing proton exchange membrane fuel cell (PEMFC) vehicles on a small scale (~3000 vehicles/year production), an additional reduction in Pt catalyst loading must be pursued for successful commercialization. The Pt loading can be reduced by employing novel higher-activity catalysts and high-gas-permeability ionomers, thereby improving the Pt utilization and optimizing gas diffusion layer and flow structures, for example.

The rotating disk electrode (RDE) technique is the most commonly used half-cell technique to screen the ORR activity of novel PEMFC catalysts synthesized on the mg-scale as well as to study the ORR kinetics on bulk catalyst surfaces and nanoparticle catalysts.[1,2] In the RDE technique, a disk working electrode is dipped into a diluted acid electrolyte and is rotated to establish a laminar flow at the electrode surfaces to control O_2 mass transport.[3] **Figure 1** illustrates the linear O_2 diffusion model on a catalyst-electrolyte interface for (a) PEMFC catalyst layers, where O_2 diffuses through gas pores and thin (~5 nm) ionomer film and that for (b) a hydrodynamic method, such as RDE, where O_2 diffuses through a thick (15 μm at 1600 rpm) diffusion layer in an electrolyte solution (with an optional ionomer film).[4,5] Assuming a simple linear diffusion model, as shown in Fig. 1, throughout the entire electrode surface and potential range, the Koutecký-Levich (K-L) equation may be used to extract kinetic currents (i_k) from the measured raw currents (i) and O_2 diffusion-limiting currents (i_{lim}), as follows:[3]

$$\frac{1}{i} = \frac{1}{i_k} + \frac{1}{i_{lim}} . \quad (1)$$

In a system such as PEMFC catalyst layers, the i_{lim} term is often negligible in studying kinetics at low-current (high-potential) regions due to fast O_2 diffusion. However, in RDE, O_2 diffusion is slow but well controlled, and thus i_k can be estimated using Eq. (1). When the electrode surface is directly in contact with the electrolyte solution, i_{lim} in Eq. (1)

equals i_d, which is the O_2 diffusion-limiting current through the diffusion layer:

$$i_d = 0.62\, nFAD_{bulk}^{2/3} C_{bulk} \nu^{-1/6} \omega^{1/2}, \quad (2)$$

where n is the number of electrons transferred through the ORR, F is Faraday's constant, A is the geometrical surface area of the working electrode, C_{bulk} and D_{bulk} are the concentration and the diffusion coefficient of O_2 in the electrolyte solution, respectively, ν is the kinematic viscosity of the solution, and ω is the rotation speed of the electrode. Here, ω, and hence i_d, can be easily controlled. In addition, i_k may be obtained from the intercept (infinite ω) in a i^{-1} vs. $\omega^{-1/2}$ plot (K-L plot).[3] Due to the low permeability of oxygen and the thick diffusion layer in a diluted acid electrolyte, kinetic information for the ORR can only be obtained in a narrow potential range (typically > 0.7–0.8 V vs. RHE in 0.1 M $HClO_4$). The ORR specific activity (SA, $\mu A/cm^2_{Pt}$) can be determined from i_k and the electrochemical surface area (ECA), and the mass activity (MA, mA/mg_{Pt}) can be determined from i_k and Pt loading.[6]

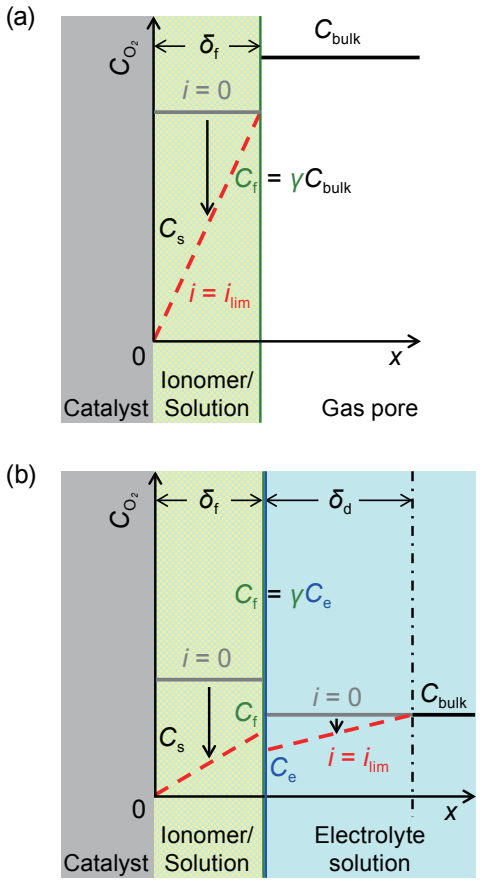

Fig. 1 Schematic diagram of a catalyst-electrolyte interface depicting the well-known linear O_2 diffusion model that can be represented by the K-L equation. The dotted line (red) represents O_2 concentration gradients in both bulk electrolyte and film. (a) O_2 diffusion in gas pores and thin electrolyte film, e.g., floating electrode and PEMFC. (b) O_2 diffusion in an electrolyte solution for controlled diffusion lengths, e.g., poly-Pt RDE with a Nafion film. Here, δ_d is the diffusion layer thickness in bulk electrolyte, and δ_f is the thin electrolyte film thickness. In addition, C_{bulk}, C_e, C_f, and C_s are the O_2 concentrations in the bulk, in the electrolyte solution at the solution-film interface, in the electrolyte film at the solution-film interface, and at the catalyst surface, respectively. Finally, γ is the partition coefficient between bulk and film phases, and i_{lim} is the O_2 diffusion-limiting current.

Ionomers such as Nafion are typically used to effectively mix nanoparticle catalyst ink and also bind catalysts on disk GC substrates.[1,7-10] In such cases, the electrode surfaces are considered to be covered with ionomer film (Fig. 1(b)). Then, i_{lim} may be expressed as follows:

$$\frac{1}{i_{lim}} = \frac{1}{i_d} + \frac{1}{i_f}, \quad (3)$$

where i_f is the O_2 diffusion-limiting current through the ionomer film.[7,11]

In this paper, we first report the preparation of the RDE apparatus, the protocols, and the catalyst film preparation method that allow us to obtain accurate and reliable ORR activity values for PEMFC catalysts. Then, we report the effect of Pt particle size and Nafion ionomer on the ORR activity for practical Pt/C catalysts evaluated by using the determined preparation method and protocols.

2. ORR Activity Measurement Using RDE

Although the RDE technique is the most commonly used method to evaluate the ORR activity for electrocatalysts in small quantities, reported baseline activity values for reference materials, such as commercial bulk polycrystalline-Pt (poly-Pt) and Pt/C catalysts, significantly vary between labs. In the following two subsections, we discuss key aspects to obtain accurate and reproducible ORR activity using the RDE technique.

2. 1 Effect of Impurity and Protocols[5]

The impurity level in an electrochemical system (cell glassware and electrolyte) and the protocols used to evaluate the ORR activity alter the measured ORR activity. The protocols include, but are not limited to: i) conditioning/break-in, ii) direction of potential sweep, iii) potential range of sweep, and iv) sweep rate. In addition, the inclusion/omission of corrections (solution resistance, background current) and the ECA estimation method change the estimated ORR activity. We systematically studied the impact of these parameters on the ORR activity to obtain accurate and reproducible ORR activity values and report the effect of the impurity level and of protocols i) through iv) in this paper.

An in-house electrochemical cell (**Fig. 2**) having a volume of 130 mL was used in all RDE measurements in this paper. Platinized Pt gauze having a surface area of > 100 cm^2 was used as a counter electrode (CE). A reversible hydrogen reference electrode (RHE) was used to avoid trace anion contamination, such as Cl^- contamination from the reference electrode (RE). The RHE was positioned close to the working electrode (WE) using a Luggin capillary tip. A poly-Pt electrode was used as the WE. Because of the small surface areas (roughness factor ~1.5) and high intrinsic activity, poly-Pt electrodes qualify as a valuable sensor of trace impurity levels in the electrochemical system that adsorb on and poison active ORR sites. In addition, due to their robustness and surface reproducibility, poly-Pt electrodes are suitable to study protocols that require repeated measurements. Electrolyte solution resistance (R_{soln}) between the RE and WE was obtained from the high frequency resistance (HFR) of electrochemical impedance spectra (EIS) and was used to correct for iR_{soln} drop.[12] The *I-E* curves under N_2 were measured using identical experimental parameters (scan rate, direction, and rotation rate) and were used to subtract background current from *I-E* curves under O_2 to obtain the ORR current.[13] Electrochemical surface area was estimated from H_{UPD} charge using 210 μC/cm^2_{Pt}.[14-17] The H_{UPD} charge was obtained from H adsorption current observed between ~0.05 V (inflection point) and ~0.4 V (double layer region) in the third cycle of cyclic voltammogram (CV) measured at 0.025–1.0 V and 20 mV/s under a N_2 atmosphere. The SA and MA were reported at 0.9 V, as conventionally reported in the literature.[6]

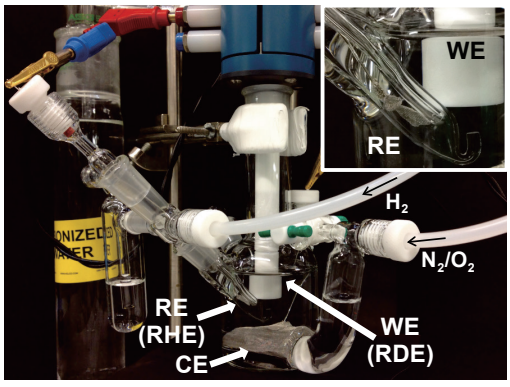

Fig. 2 Photograph depicting the in-house electrochemical cell system.

An appropriate cleaning procedure for the RDE apparatus is necessary to avoid both organic and inorganic contamination, which can lower the measured ORR activity. The cell glassware and components were soaked in concentrated sulfuric acid followed by an overnight soak in Nochromix solution. Subsequently, the cell glassware and components were rinsed thoroughly and boiled in DI water. The change in SA of poly-Pt (**Fig. 3(**a)) extracted from the ORR *I-E* curves (Fig. 3(c)) illustrates the continuous elimination of impurities in the cell glassware during the rinsing and boiling. In this instance, boiling in DI water one time resulted in a close-to-maximum value of SA (~3 mA/cm^2_{Pt}). Correspondingly, on the CVs obtained under N_2 (Fig. 3(b)), a slight positive shift in the onset of oxides as well as more pronounced peaks in the H_{UPD} regime near 0.3 V related to anion adsorption become no longer noticeable after boiling in DI water. Since the cleanliness level reachable after the first boiling may depend on the skill of experimenters, additional rinsing in boiling water is recommended.

Perchloric acid is commonly used to minimize the impact of anion adsorption on the ORR activity because perchlorate is only weakly adsorbed on Pt surfaces.[18] However, because commercially available perchloric acid sources contain trace impurities (0.1–10 ppm) of chloride, sulfate, phosphate, and nitrate ions, which are known to lower the ORR activity, and the concentration depends on the grade, the choice of grade can impact the measured ORR activity.[19] As shown in **Fig. 4**, two of the grades tested resulted in

significantly low measured ORR activity, whereas the other six grades yielded similar values. Since Veritas® Doubly Distilled exhibits the highest ORR activity, and hence is expected to contain the least amount of contaminants, we used Veritas® Doubly Distilled in our RDE studies.

Before evaluating the ORR activity, it is necessary to conduct a conditioning procedure to reach maximum catalyst utilization. **Figure 5**(a) illustrates the stabilization of the signature H_{UPD} and oxide features on poly-Pt, which indicates completion of conditioning, through repetitive surface oxidation/reduction cycles that effectively remove certain contaminants.

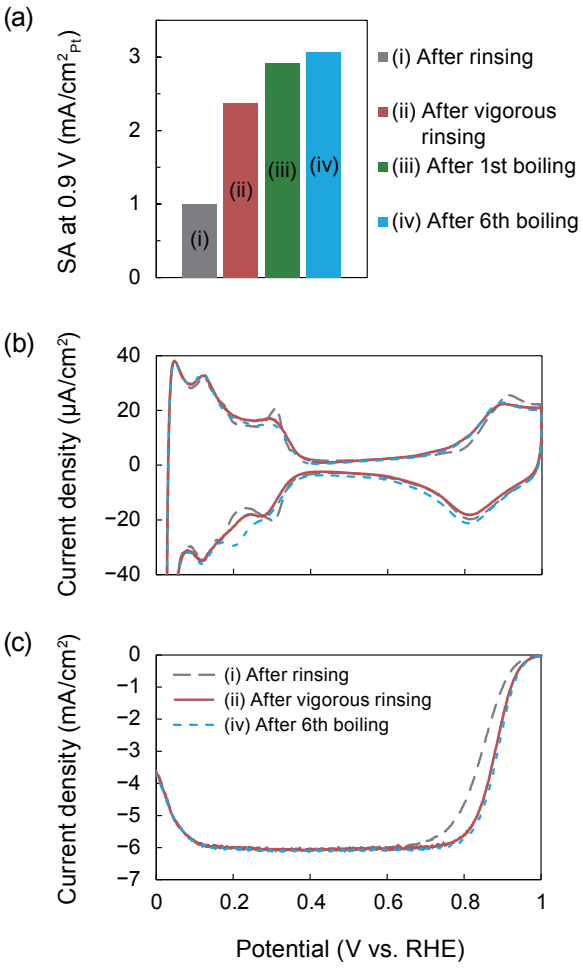

Fig. 3 Impact of removal of impurities at several intermediate stages of cleaning: (a) SA at 0.9 V obtained from (c), (b) CVs measured under N_2, (c) ORR *I-E* curves after background correction. All ORR *I-E* measurements for poly-Pt conducted in 0.1 M $HClO_4$ under the conditions of 20 mV/s, 1600 rpm, −0.01 to 1.0 V, anodic sweep, and iR_{soln} correction.

Figure 5(b) depicts the corresponding change in the ORR *I-E* curve profiles before and after conditioning. Based on our study, the upper potential at 1.2 V appears

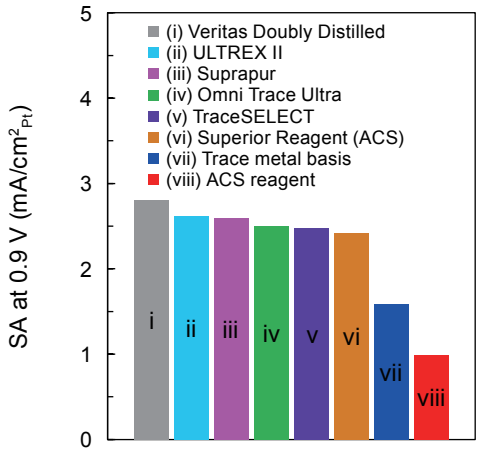

Fig. 4 Effect of impurity level ($HClO_4$ grade) on the SA of poly-Pt at 0.9 V in 0.1 M $HClO_4$ measured under the conditions of 20 mV/s, 1600 rpm, −0.01 to 1.0 V, and anodic sweep.

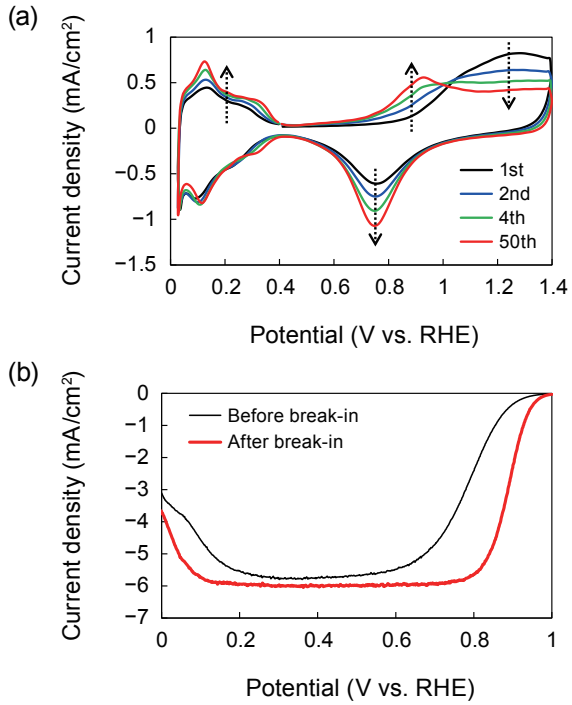

Fig. 5 Effect of conditioning of poly-Pt: (a) CVs measured under N_2 during conditioning (0 rpm), (b) ORR *I-E* curves before and after conditioning (20 mV/s, 1600 rpm, −0.01 to 1.0 V, anodic sweep, iR_{soln} and background correction). All measurements were conducted in 0.1 M $HClO_4$.

to achieve complete conditioning for both the poly-Pt and carbon-supported Pt catalysts.

The effect of potential range and scan direction on the ORR *I-E* curves is inseparably linked. As shown in **Fig. 6**(a), we altered the lower potential limit in the range of −0.01 to 0.5 V, while the scan rate and upper potential (E_{high}) were fixed at 20 mV/s and 1.0 V, respectively. Figure 6(b) demonstrates the effect of lower potential (E_{low}) on the SA for three consecutive sweeps in the anodic direction. When the E_{low} is at potentials of > 0.1 V, the Pt surface is not completely reduced between sweeps, leading to a build-up of oxides and an accompanying loss in measured SA with each consecutive cycle (No. 1, 2 and 3). When the E_{low} is at potentials of < 0.1 V, the sweeps start with an oxide-free surface, leading to high reproducibility among each of the three consecutive sweeps. Figure 6(c) shows the same trend for the SA measured in the cathodic direction as was observed in the anodic direction, while the magnitude of SA is lower. This result indicates that a complete removal of surface oxides is indispensable to obtain reproducible SA in the cathodic direction as well. Based on these observations, we down-select the anodic scan direction that is initiated from −0.01 V and proceeds to OCP (1.0 V).

Figure 7 illustrates the effect of scan rate on the ORR *I-E* curves for poly-Pt in the range 0.5–100 mV/s. The *I-E* profile in the kinetic and mixed kinetic/mass transport regime declines systematically with a decrease in scan rate. Although the ORR *I-E* curves for poly-Pt remain within a narrow band for scan rates of ≥ 10 mV/s, a large shift to less positive potential is observed at scan rates of ≤ 5 mV/s. At even lower scan

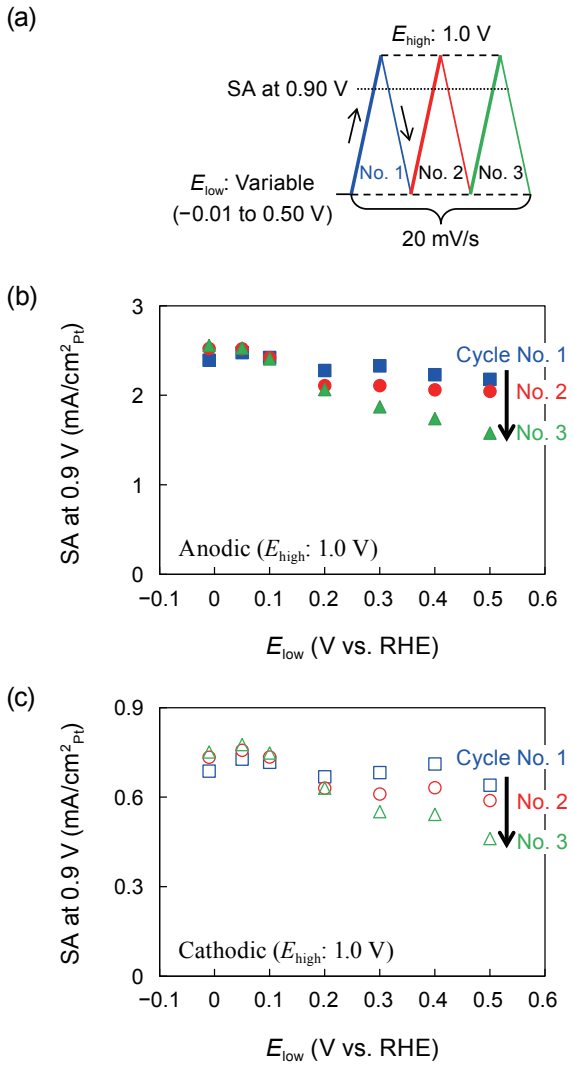

Fig. 6 (a) Potential profiles used to evaluate the effect of E_{low} on the SA at 0.9 V in 0.1 M $HClO_4$ (E_{high}: 1.0 V, background and iR_{soln} correction). SA of poly-Pt electrode as a function of E_{low} for (b) three anodic sweep profiles and (c) three cathodic sweep profiles.

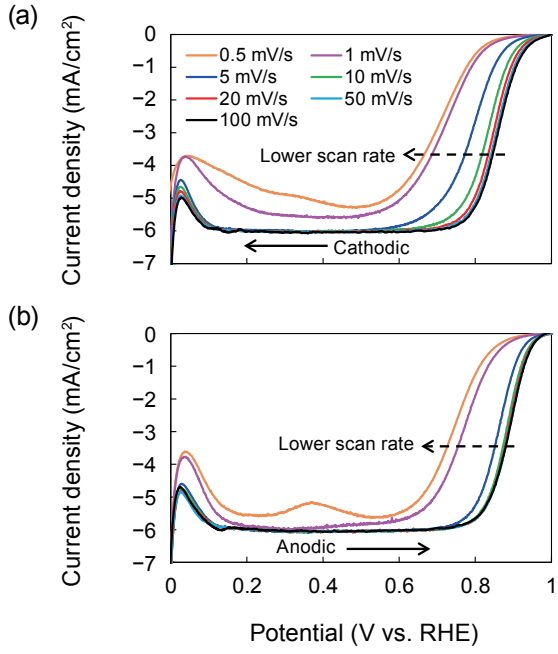

Fig. 7 ORR *I-E* curves of poly-Pt in 0.1 M $HClO_4$ at 0.5–100 mV/s without background correction: (a) cathodic scan and (b) anodic scan. Sweeps were initiated from −0.01 V and swept anodically to 1.0 V followed by a cathodic sweep to −0.01 V under the conditions of 1600 rpm and iR_{soln} correction.

rates, such as 0.5 and 1 mV/s, additional lowering of the limiting current as well as a divergent feature are observed. These features may be attributed to impurity anion adsorption and H_2O_2 production, which impede the extraction of reliable SA values. At higher scan rates of > 20 mV/s, the contribution of background correction on the SA is not minor for Pt/HSC. Based on these considerations for contamination and background correction contributions at high scan rates, we can narrow down the favored range of scan rates to 10–20 mV/s. Since 20 mV/s is fairly common in the literature, we may further down-select to 20 mV/s.[6,20-22] The established experimental system and protocols in the current section were applied to all of the experiments described in this paper.

2. 2 Effect of Catalyst Film Thickness and Uniformity[23]

The thin-film RDE (TF-RDE) technique is a derivative of the RDE technique that is used to study the ORR activity for practical nanoparticle catalysts, in which catalyst thin film is formed on a disk GC substrate by depositing catalyst ink followed by drying.[1,7] Since the catalyst film has a finite thickness with imperfect uniformity, additional care must be taken for catalyst film preparation to extract ORR kinetics without hindrance from O_2 diffusion or proton transfer resistances within the catalyst film.[24] In addition, Nafion ionomer, which is commonly used in the literature, may impact the ORR activity on Pt-based nanoparticle catalysts, as reported for extended Pt-based catalyst surfaces.[25,26] Although not required for proton conduction in an RDE system, Nafion is incorporated in order to well disperse the catalyst ink and/or immobilize catalysts on the GC either by mixing with the catalyst ink or by acting as a cap over the dried catalyst film on the GC disk.[1,7-10]

In an attempt to obtain intrinsic ORR activity on practical Pt/C catalysts with high reproducibility, we fabricated catalyst films of Pt/HSC and Pt/V (Vulcan) using different ink formulations and drying processes. The ink formulations discussed herein may be classified as Nafion-based (N) or Nafion-free (NF) formulations. The accompanying film drying processes may be described as stationary (S), rotational (R), air drying (AD), or IPA atmosphere drying (IPAD). The nomenclature for the different combinations of ink formulation and film drying can thus be represented by the following acronyms: i) Nafion-based stationary air drying (N-SAD), ii) Nafion-free stationary air drying (NF-SAD), iii) Nafion-based rotational air drying (N-RAD), and iv) Nafion-free stationary IPA drying (NF-SIPAD).

For N-SAD and N-RAD techniques, catalyst inks were prepared by sonicating 7.6 mg of Pt/C catalyst powder with 7.6 mL of DI water, 2.4 mL of IPA, and 40 μL of 5 wt% Nafion solution in an ice bath.[27] For the N-SAD technique, a 10-μL aliquot of ink (18 $\mu g/cm^2_{Pt}$) was pipetted onto the GC and air dried at 40°C in an oven. For the N-RAD technique, the aliquot of ink was pipetted onto the GC tip mounted to an inverted rotator shaft (while gently spinning at 0–100 rpm).[9] The rotator speed was gradually raised to 700 rpm, and the ink was allowed to dry for 15 min in air at 23±2°C.

For the NF-SAD technique, Pt/HSC catalyst inks were prepared with 7.6 mg of catalyst powder, 6.5 mL of DI water, 3.5 mL of IPA, and 2.5 μL of 10-times diluted TRITON X-100.[27] Here, Pt/V catalyst inks were prepared with no added surfactant. A 10-μL aliquot of ink (18 $\mu g/cm^2_{Pt}$) was pipetted onto the GC and air dried at 40°C in an oven.

For the NF-SIPAD technique, Pt/C catalyst inks were prepared with 3.8 mg of catalyst powder, 7.6 mL of DI water, and 2.4 mL of IPA. A 5-μL aliquot of ink (4.5 $\mu g/cm^2_{Pt}$) was pipetted onto the GC disk in a beaker filled with a small amount of IPA. The beaker was then sealed with a perforated polymer film, and the ink was gradually (~3 hours) dried under IPA vapor (~13 kPa) at 40°C.[28]

Figure 8 depicts SEM images of tilted catalyst film on GC substrates fabricated using N-SAD, N-RAD and NF-SIPAD. The catalyst film fabricated using N-SAD was non-uniform with a thick coffee-ring structure at the periphery of the GC, while a limited quantity of catalysts was deposited on the rest of the central GC area. The catalyst film fabricated using N-SAD was also non-uniform, but the coffee-ring structure was less pronounced and more catalysts were deposited on the rest of the central GC area, as compared to the catalyst film fabricated using the N-SAD technique. In contrast, the catalyst films fabricated using NF-SIPAD were thin and highly uniform.

The representative ORR *I-E* profiles for Pt HSC catalyst films fabricated using the four methods as well as poly-Pt are shown in **Fig. 9**. The Tafel

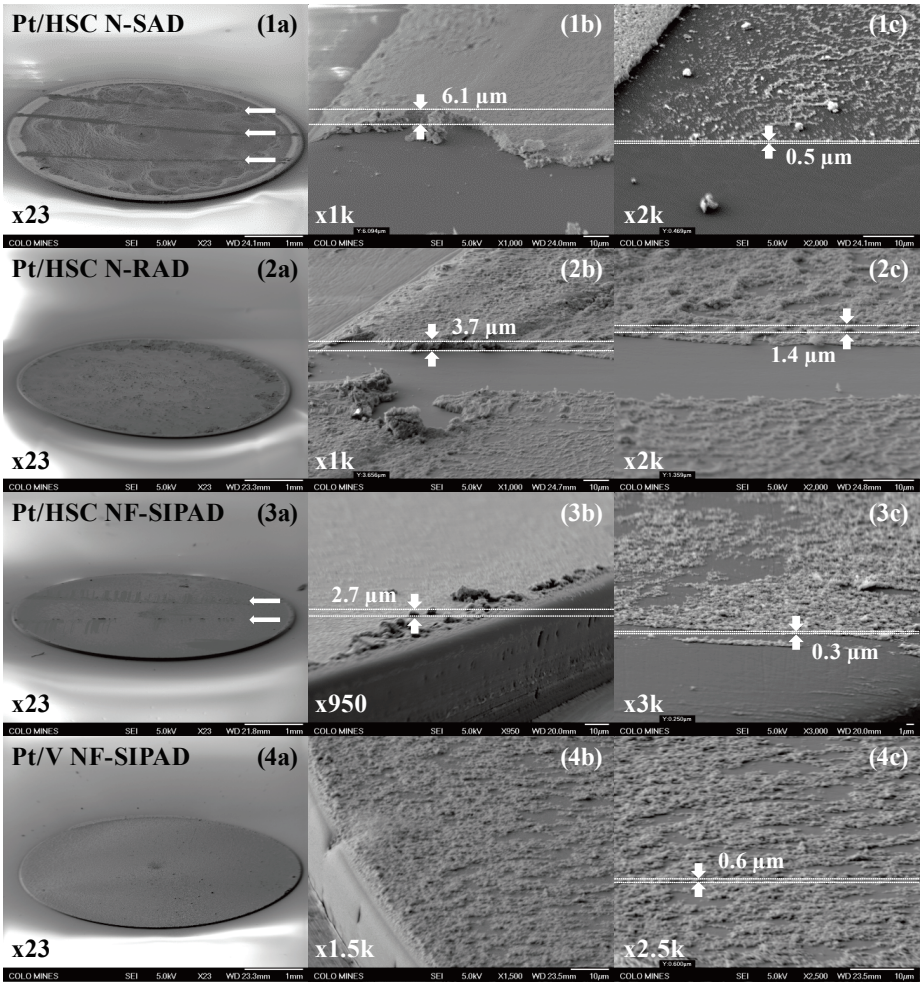

Fig. 8 SEM images of catalyst films: Pt/HSC (1) N-SAD, (2) N-RAD, (3) NF-SIPAD, (4) Pt/V NF-SIPAD, (a) entire or half area, (b) edge area, (c) near edge area. Catalyst was removed over a narrow band (horizontal arrows) to facilitate observation and analysis of catalyst layer thickness for each local area.

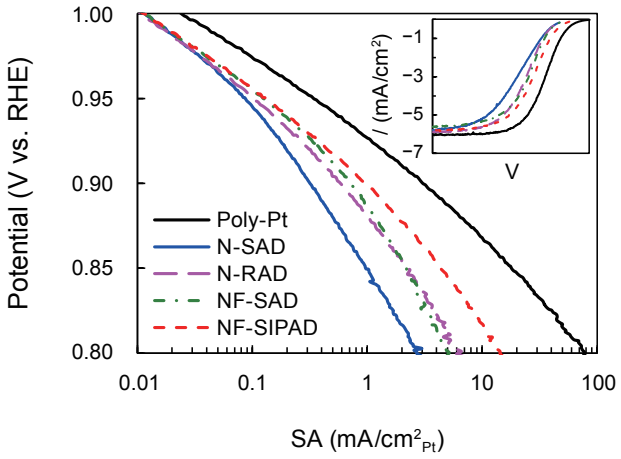

Fig. 9 ORR Tafel plots of poly-Pt and Pt/HSC catalyst layers fabricated using N-SAD, NF-SAD, N-RAD and NF-SIPAD techniques. ORR activity measured in 0.1 M $HClO_4$ under the conditions of 1600 rpm, 20 mV/s, −0.01 to 1.0 V, and anodic sweep.

curve for the thin uniform film fabricated using the NF-SIPAD technique closely resembles that for poly-Pt in the kinetic regime with a slight deviation in transition from the mixed kinetic/diffusion regime to the O_2 diffusion-limiting current (inset of Fig. 9). A profile resembling that of poly-Pt, which is a catalyst film with approximately zero thickness, indicates that the measured activity loss due to O_2 diffusion within the catalyst film is negligible for the thin uniform film (NF-SIPAD) at low current densities (0.9 V), where ORR activity values are reported. Therefore, it would be reasonable to consider that thin uniform films fabricated by the NF-SIPAD technique allow us to extract intrinsic ORR activity for practical Pt/C catalysts. In contrast, for the thick non-uniform catalyst film fabricated by the conventional N-SAD technique, the *I-E* profile departs significantly from the poly-Pt profile. The sources of the departure could be O_2 diffusion resistance and proton transfer resistance ($R_{H^+,\,cl\text{-}eff}$) within the catalyst film and ionomer adsorption/blocking. **Figure 10** illustrates the magnitude of the losses associated with each source for the N-SAD, N-RAD, and NF-SAD techniques determined using EIS. The gray bars correspond to activity values corrected for the solution resistance, O_2 diffusion within a diffusion layer in an acid solution, and background current. For the Nafion-free thin uniform film fabricated by the NF-SIPAD technique, the losses due to O_2 diffusion resistance within the catalyst film as well as $iR_{H^+,\,cl\text{-}eff}$ at 0.9 V are negligibly small. Thus, we treat the value presented in gray for the NF-SIPAD technique as the intrinsic ORR activity of the Pt/HSC catalyst and account for any deviation from this value as measured activity loss. For the catalyst film fabricated by the NF-SAD technique, the $iR_{H^+,\,cl\text{-}eff}$ loss (orange) is no longer negligible. The residual loss (blue) is attributable to O_2 diffusion. The magnitude of the loss due to ionomer adsorption/blocking can be separated as follows. Catalyst films fabricated by the NF-SAD and N-RAD techniques (18 $\mu g/cm^2_{Pt}$) have almost identical values of $R_{H^+,\,cl\text{-}eff}$. Since both $R_{H^+,\,cl\text{-}eff}$ and O_2 diffusion resistance are functions of catalyst film thickness, the two films should suffer from almost identical O_2 diffusion losses. The residual difference between these two techniques can then be attributed to ionomer adsorption/blocking losses (green). Catalyst film fabricated by the conventional N-SAD technique exhibits only one third of the intrinsic activity. Since catalyst films fabricated by the N-RAD and N-SAD techniques are expected to have the same ionomer related loss (I/C 0.5), the additional loss for the N-SAD technique can be attributed to the enhanced O_2 diffusion loss that stems from the thicker coffee-ring structure (Fig. 8). As depicted in **Fig. 11**, the measured SA increase from the N-SAD technique to the NF-SIPAD technique depends on the catalyst

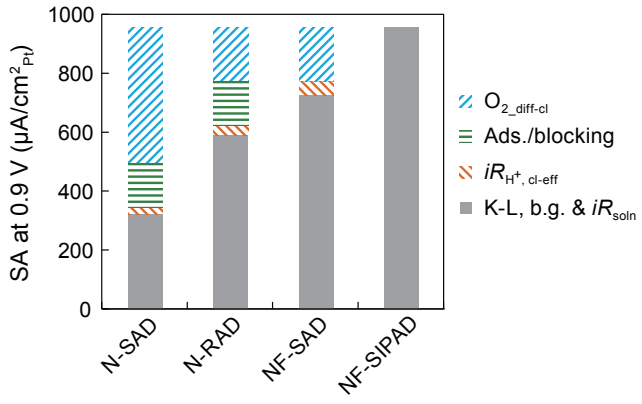

Fig. 10 Breakdown of SA losses at 0.9 V for Pt/HSC catalyst layers fabricated using N-SAD, N-RAD, NF-SAD and NF-SIPAD techniques. N-RAD and NF-SAD catalyst layers had identical thickness, and N-SAD and N-RAD layers had identical I/C ratios.

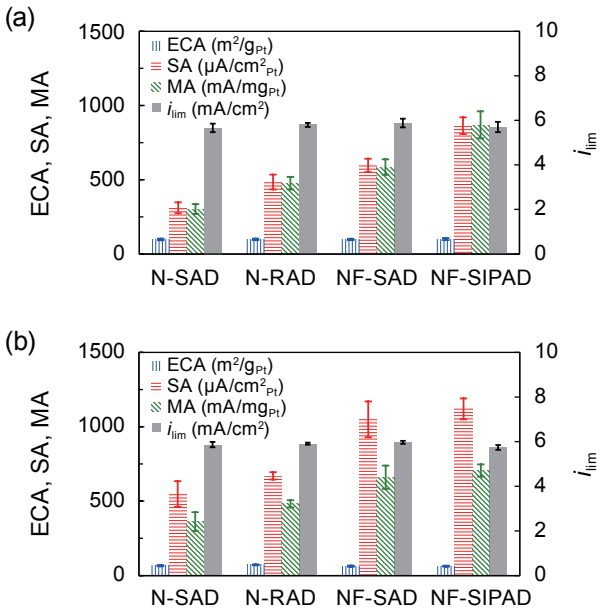

Fig. 11 ECA, SA and MA at 0.9 V in 0.1 M $HClO_4$ for (a) Pt/HSC, and (b) Pt/V catalyst layers fabricated using N-SAD, NF-SAD, N-RAD, and NF-SIPAD techniques for 20–49 independent samples.

(2.8-fold higher for Pt/HSC and 2.0-fold higher for Pt/V). The difference in the SA increase between catalysts indicates that ORR activity comparison conducted using catalyst films fabricated by the conventional N-SAD technique can be misleading. Therefore, Nafion-free thin uniform catalyst films are essential in order to evaluate and fairly compare ORR activity values.

3. Effect of Pt Particle Size on ORR Activity[29]

Further reduction of Pt loading requires an understanding of the impact of Pt particle size on the ORR activity/performance and durability. Specifically, the 'particle size effect' for the ORR activity on Pt-based catalysts has been debated for over 50 years.[6,13,30-44] In most of the studies in the literature, less-refined RDE techniques were used to obtain the ORR activity for practical nanoparticle Pt catalysts.[6,13,43] Since less-refined RDE techniques can lead to unreliable activity evaluation, we re-evaluated the particle size effect using commercial Pt/C catalysts using well-dispersed, Nafion-free thin uniform catalyst layers as well as well-defined protocols.

The SA values obtained herein, as well as values reported in the literature, are plotted in **Fig 12**. Since the particle size of practical Pt/C catalysts has a finite distribution, we use the average particle size calculated from H_{UPD} to discuss the particle size effect. Compared to the SA values reported in the literature (0.2–0.5 mA/cm$^2_{Pt}$) using practical Pt catalysts in the range of approximately 2 to 10 nm, the values obtained in our study (filled blue circles) were significantly higher (0.74–1.8 mA/cm$^2_{Pt}$).[6,13] In contrast, the SA values in our study are comparable with those of Perez-Alonso et al.,[44] who used model electrodes in which a thin layer of Nafion-free Pt nanoparticles were deposited directly onto GC substrates by a sputtering technique (sputtered Pt/GC). Since the SA values in our study fall in the same range as those of Perez-Alonso et al.,[44] which have negligible loss due to O_2 diffusion, it is reasonable to consider the high SA values obtained in our study as approaching the 'intrinsic' activity of Pt nanoparticles. In order to compare these results with the results obtained using the theoretical model, the SA in Fig. 12 was normalized to poly-Pt SA for each data set and re-plotted in **Fig. 13**.[6,13,42,44,45] The results of a theoretical study by Tritsaris et al.[42] (a truncated octahedral particle model with dissolved edges and corners) are shown by black squares with a broken line. The SA value at ~30 nm evaluated by our group using a Nafion-free Pt nanotube thin catalyst layer (blue open circle) is also shown in Fig. 13.[45] In studies that used less refined TF-RDE techniques,[6,13] the SA remains low in the range of < 10 nm, but increases significantly in the range from ~10 nm to bulk poly-Pt. However, in our study, SA rapidly increases in the range from ~2 nm to ~10 nm, followed by an attenuated increase and plateau reaching bulk poly-Pt activity. The trend in our study coincides with most of the sputtered Pt/GC data and closely agrees with the theoretical model that assumes truncated octahedral particles with active terrace sites.

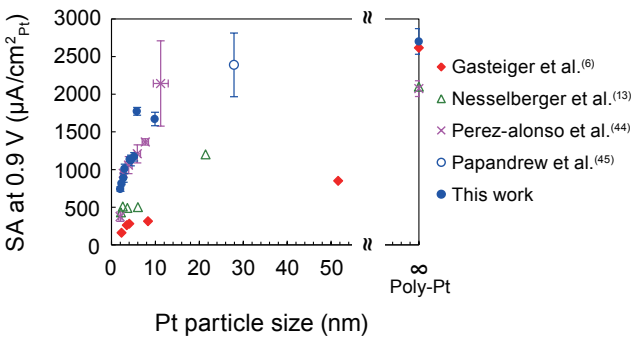

Fig. 12 Particle size dependence of specific activity at 0.9 V vs. RHE in 0.1 M $HClO_4$ obtained in this study and in the literature.

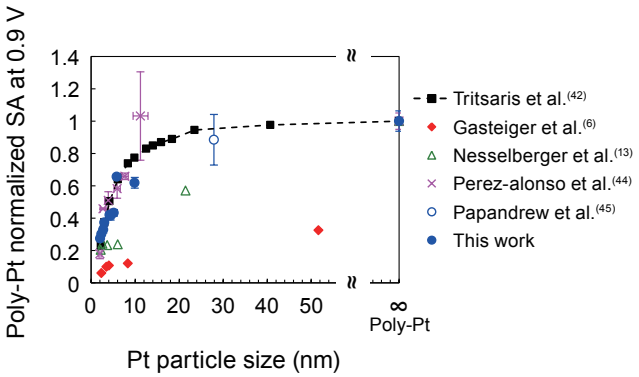

Fig. 13 Normalized SA dependence on particle size effect obtained in our study and through experimental and theoretical studies in the literature. The dashed black line indicates the trend for the theoretically determined discrete values represented by the black squares.

4. Impact of Nafion Ionomer on ORR Activity[46]

Ionomers such as Nafion are essential to providing sufficient proton paths to facilitate facile fuel cell reactions in PEMFCs. However, recent studies using the RDE technique have report that Nafion lowers the ORR activity on extended catalyst surfaces such as single-crystal Pt and poly-Pt.[26,47-49] In this section, we discuss the impact of Nafion on the ORR activity for practical Pt/C catalysts (Pt/HSC, Pt/V: Vulcan, Pt/LSC: low-surface-area carbon) by using well-dispersed Nafion-free catalyst layers and poly-Pt and applying thin Nafion films (~10 nm) to the electrode surfaces by capping with Nafion ionomer.

CVs obtained under N_2 and ORR Tafel plots for 46 wt% Pt/HSC and 48 wt% Pt/LSC are shown in **Figs. 14**(a) through (d) as examples illustrating two extreme cases of carbon support. In Fig. 14(a), 46 wt% Pt/HSC exhibits no clear shifts in the H_{UPD} regime or onset potential shifts in the oxide-formation/reduction regime. Correspondingly, in Fig. 14(b), shifts in the ORR Tafel curves are not clearly observable until the I/C ratio becomes high (I/C ≥ 1.5). In contrast, in Fig. 14(c), 48 wt% Pt/LSC exhibits observable peak shifts in the H_{UPD} region and a slight shift in the onset potential of the oxide-formation regime with increasing I/C ratio. In the ORR Tafel curves (Fig. 14(d)), larger shifts are observed with increasing I/C ratio.

The impact of Nafion on the ORR activity for Pt/HSC, Pt/V, and Pt/LSC is illustrated in **Fig. 15**. The SA values were normalized with the value at I/C ≈ 0 for each catalyst. Carbon-surface-area-specific Nafion loading (first abscissa) was estimated from the I/C ratio and the BET surface area of carbon supports: HSC, Vulcan ≈ 250 m^2/g, and LSC ≈ 80 m^2/g. The Nafion film thickness (second abscissa) was also estimated using the BET surface areas assuming uniform Nafion coverage. Although the actual BET surface area of HSC is ~800 m^2/g, we used 250 m^2/g based on the following understanding: i) HSC and Vulcan have similar carbon particle sizes, ii) Pt particles are located both on the outer surface of HSC particles and within the pores of the HSC,[50-52] and iii) only Pt particles located on the outer surface of the HSC support are in contact with the ionomer.[51-53] For Pt/V and Pt/LSC catalysts, similarly large SA losses are

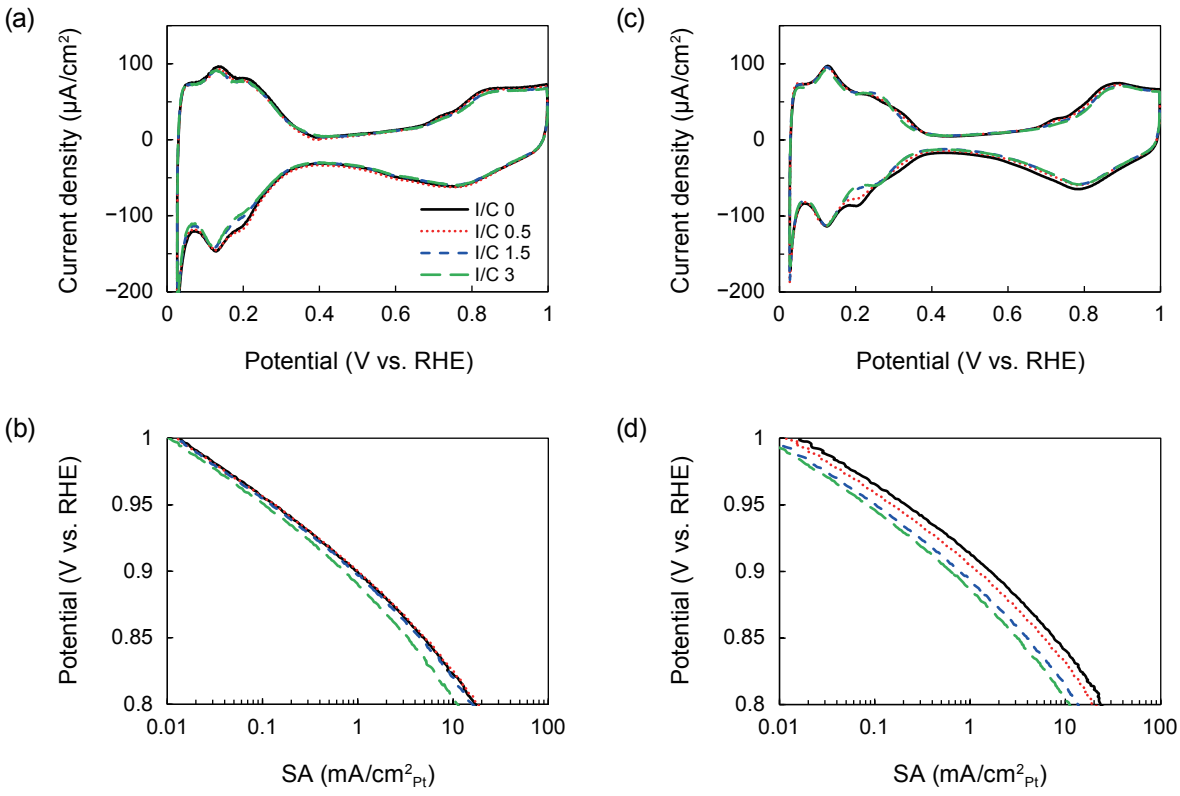

Fig. 14 Effect of I/C ratio on (a), (c) CVs measured under N_2 and (b), (d) ORR *I-E* curves in 0.1 M $HClO_4$ at 20 mV/s for (a), (b) 46 wt% Pt/HSC and (c), (d) 48 wt% Pt/LSC.

observed with increasing Nafion loadings/thickness to ~1 μg/cm$^2_{carbon}$/~5 nm, and the SA then reaches a plateau (red band). In contrast, for Pt/HSC catalysts, the SA loss by the plateau is relatively small. Notably, the Nafion thickness at which the normalized SA starts to plateau corresponds to the minimum Nafion thickness of ~5 nm reported in a microscopic study,[54] which revealed that Nafion non-uniformly covers the carbon support with a minimum thickness of ~5 nm and that Nafion coverage increases with increasing Nafion loadings. In Fig. 15, this study shows that Nafion coverage decreases with decreasing loadings from ~1 μg/cm$^2_{carbon}$ (~5 nm in thickness) and can reach unity at loadings greater than 1 μg/cm$^2_{carbon}$. Since the SA decreases in the loading range in which the coverage increases and reaches a plateau at the loading where the coverage approaches unity, it is reasonable to interpret that Nafion coverage dominates the SA loss. This interpretation is supported by the observation that normalized SA values for Nafion-capped poly-Pt (coverage ~1),[26] Pt/V, and Pt/LSC in the plateau region are comparable. Therefore, the attenuated SA loss for Pt/HSC catalysts by the plateau is reasonably understood as follows: Pt particles shielded from Nafion in micropores of HSC support maintain their original activities.[51-53]

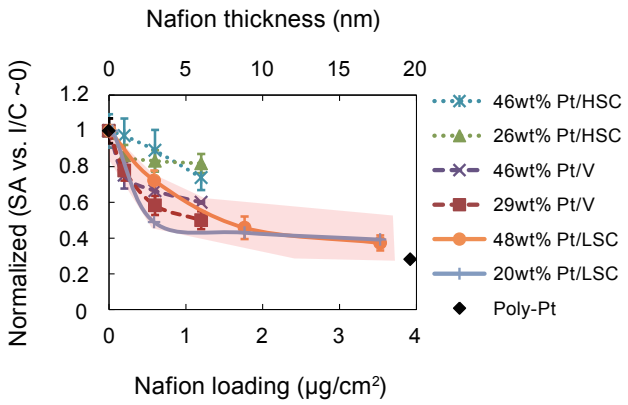

Fig. 15 Nafion loading dependence of the normalized SA at 0.9 V for Pt/C nanoparticle catalysts as well as bulk poly-Pt. Nafion loading/thickness estimated from actual roughness factor for poly-Pt. Error bars indicate normalized standard deviation for catalysts tested using four or more samples (46 wt% and 26 wt% Pt/HSC, 29 wt% Pt/V, and 48 wt% Pt/LSC), and normalized maximum and minimum SA for catalysts tested using less than four samples (46 wt% Pt/V).

5. Summary

Our study revealed that the cleanliness of the RDE apparatus and proper RDE protocols are essential for accurate and reproducible ORR activity measurement using the RDE technique. In addition, for practical nanoparticle catalyst evaluation, fabrication of thin and uniform catalyst films is important in order to minimize the impact from O_2 diffusion and proton transfer resistance within catalyst films. We demonstrated that Nafion-free thin uniform catalyst films allowed us to extract "intrinsic" activity and thus fairly compare activity values. Based on these understandings, the effect of Pt particle size was re-evaluated. Unlike previous studies that used conventional Nafion-based thick non-uniform catalyst films, our results agreed well with a truncated octahedral particle model that assumes active terrace sites. The impact of Nafion ionomer on the ORR activity was also studied for practical Pt/C catalysts using the refined RDE technique. It was found that Nafion lowers the ORR activity and the extent of activity decrease depends on Nafion coverage.

References

(1) Gloaguen, F. et al., "Kinetic Study of Electrochemical Reactions at Catalyst-recast Ionomer Interfaces from Thin Active Layer Modelling", *J. Appl. Electrochem.*, Vol. 24, No. 9 (1994), pp. 863-869.

(2) Gojković, S. L. et al., "O_2 Reduction on an Ink-type Rotating Disk Electrode Using Pt Supported on High-Area Carbons", *J. Electrochem. Soc.*, Vol. 145, No. 11 (1998), pp. 3713-3720.

(3) Bard, A. J. and Faulkner, L. R., *Electrochemical Methods: Fundamentals and Applications* (2000), 833p., John Wiley.

(4) Zecevic, S. K. et al., "Kinetics of O_2 Reduction on a Pt Electrode Covered with a Thin Film of Solid Polymer Electrolyte", *J. Electrochem. Soc.*, Vol. 144, No. 9 (1997), pp. 2973-2982.

(5) Shinozaki, K. et al., "Oxygen Reduction Reaction Measurements on Platinum Electrocatalysts Utilizing Rotating Disk Electrode Technique: I. Impact of Impurities, Measurement Protocols and Applied Corrections", *J. Electrochem. Soc.*, Vol. 162, No. 10 (2015), pp. F1144-F1158.

(6) Gasteiger, H. A. et al., "Activity Benchmarks and Requirements for Pt, Pt-alloy, and Non-Pt Oxygen Reduction Catalysts for PEMFCs", *Appl. Catal. B: Environ.*, Vol. 56, No. 1-2 (2005), pp. 9-35.

(7) Schmidt, T. J. et al., "Characterization of High-surface-area Electrocatalysts Using a Rotating Disk Electrode Configuration", *J. Electrochem. Soc.*, Vol. 145, No. 7 (1998), pp. 2354-2358.
(8) Takahashi, I. and Kocha, S. S., "Examination of the Activity and Durability of PEMFC Catalysts in Liquid Electrolytes", *J. Power Sources*, Vol. 195, No. 19 (2010), pp. 6312-6322.
(9) Garsany, Y. et al., "Experimental Methods for Quantifying the Activity of Platinum Electrocatalysts for the Oxygen Reduction Reaction", *Anal. Chem.*, Vol. 82, No. 15 (2010), pp. 6321-6328.
(10) Ke, K. et al., "An Accurate Evaluation for the Activity of Nano-sized Electrocatalysts by a Thin-film Rotating Disk Electrode: Oxygen Reduction on Pt/C", *Electrochem. Acta*, Vol. 72, (2012), pp. 120-128.
(11) Gottesfeld, S. et al., "Oxygen Reduction Kinetics on a Platinum RDE Coated with a Recast Nafion Film", *J. Electrochem. Soc.*, Vol. 134, No. 6 (1987), pp. 1455-1462.
(12) Van der Vliet, D. et al., "On the Importance of Correcting for the Uncompensated Ohmic Resistance in Model Experiments of the Oxygen Reduction Reaction", *J. Electroanal. Chem.*, Vol. 647, No. 1 (2010), pp. 29-34.
(13) Nesselberger, M. et al., "The Particle Size Effect on the Oxygen Reduction Reaction Activity of Pt Catalysts: Influence of Electrolyte and Relation to Single Crystal Models", *J. Am. Chem. Soc.*, Vol. 133, No. 43 (2011), pp. 17428-17433.
(14) Gilman, S., "A Study of the Mechanism of Carbon Monoxide Adsorption on Platinum by a New Electrochemical Procedure", *J. Phys. Chem.*, Vol. 67, No. 1 (1963), pp. 78-84.
(15) Gilman, S., "Measurement of Hydrogen Adsorption by the Multipulse Potentiodynamic (mpp) Method", *J. Electroanal. Chem. (1959),* Vol. 7, No. 5 (1964), pp. 382-391.
(16) Brummer, S. B., "The Use of Large Anodic Galvanostatic Transients to Evaluate the Maximum Adsorption on Platinum from Formic Acid Solutions", *J. Phys. Chem.*, Vol. 69, No. 2 (1965), pp. 562-571.
(17) Biegler, T. and Woods, R., "Limiting Oxygen Coverage on Smooth Platinum Anodes in Acid Solution", *J. Electroanal. Chem. Interfacial Electrochem.*, Vol. 20, No. 1 (1969), pp. 73-78.
(18) Omura, J. et al., "Electrochemical Quartz Crystal Microbalance Analysis of the Oxygen Reduction Reaction on Pt-based Electrodes. Part 1: Effect of Adsorbed Anions on the Oxygen Reduction Activities of Pt in HF, $HClO_4$, and H_2SO_4 Solutions", *Langmuir*, Vol. 27, No. 10 (2011), pp. 6464-6470.
(19) Ross Jr., P. N., "Structure Sensitivity in Electrocatalytic Properties of Pt: II. Oxygen Reduction on Low Index Single Crystals and the Role of Steps", *J. Electrochem. Soc.*, Vol. 126, No. 1 (1979), pp. 78-82.
(20) Stamenković, V. et al., "Surface Composition Effects in Electrocatalysis: Kinetics of Oxygen Reduction on Well-defined Pt_3Ni and Pt_3Co Alloy Surfaces", *J. Phys. Chem. B*, Vol. 106, No. 46 (2002), pp. 11970-11979.
(21) Mayrhofer, K. J. J. et al., "Measurement of Oxygen Reduction Activities via the Rotating Disc Electrode Method: From Pt Model Surfaces to Carbon-supported High Surface Area Catalysts", *Electrochim. Acta*, Vol. 53, No. 7 (2008), pp. 3181-3188.
(22) Stephens, I. E. L. et al., "Oxygen Electroreduction Activity and X-ray Photoelectron Spectroscopy of Platinum and Early Transition Metal Alloys", *ChemCatChem*, Vol. 4, No. 3 (2012), pp. 341-349.
(23) Shinozaki, K. et al., "Oxygen Reduction Reaction Measurements on Platinum Electrocatalysts Utilizing Rotating Disk Electrode Technique: II. Influence of Ink Formulation, Catalyst Layer Uniformity and Thickness", *J. Electrochem. Soc.*, Vol. 162, No. 12 (2015), pp. F1384-F1396.
(24) Gloaguen, F. et al., "An Evaluation of the Macro-homogeneous and Agglomerate Model for Oxygen Reduction in PEMFCs", *Electrochim. Acta*, Vol. 43, No. 24 (1998), pp. 3767-3772.
(25) Subbaraman, R. et al., "Three Phase Interfaces at Electrified Metal-solid Electrolyte Systems 1. Study of the Pt (*hkl*)-Nafion Interface", *J. Phys. Chem. C*, Vol. 114, No. 18 (2010), pp. 8414-8422.
(26) Kodama, K. et al., "Catalyst Poisoning Property of Sulfonimide Acid Ionomer on Pt(111) Surface", *J. Electrochem. Soc.*, Vol. 161, No. 5 (2014), pp. F649-F652.
(27) Kocha, S. S. et al., "Influence of Ink Composition on the Electrochemical Properties of Pt/C Electrocatalysts", *ECS Trans.*, Vol. 50, No. 2 (2012), pp. 1475-1485.
(28) Yano, H. et al., "Temperature Dependence of Oxygen Reduction Activity at Nafion-coated Bulk Pt and Pt/Carbon Black Catalysts", *J. Phys. Chem. B*, Vol. 110, No. 33 (2006), pp. 16544-16549.
(29) Shinozaki, K. et al., "Re-examination of the Pt Particle Size Effect on the Oxygen Reduction Reaction for Ultrathin Uniform Pt/C Catalyst Layers without Influence from Nafion", *Electrochim. Acta*, Vol. 213 (2016), pp. 783-790.
(30) Zeliger, H. I., "Fuel Cell Performance as a Function of Catalyst Surface Area", *J. Electrochem. Soc.*, Vol. 114, No. 2 (1967), pp. 144-145.
(31) Bregoli, L. J., "The Influence of Platinum Crystallite Size on the Electrochemical Reduction of Oxygen in Phosphoric Acid", *Electrochim. Acta*, Vol. 23, No. 6 (1978), pp. 489-492.
(32) Peuckert, M. et al., "Oxygen Reduction on Small Supported Platinum Particles", *J. Electrochem. Soc.*, Vol. 133, No. 5 (1986), pp. 944-947.

(33) Sattler, M. L. and Ross, P. N., "The Surface Structure of Pt Crystallites Supported on Carbon Black", *Ultramicroscopy*, Vol. 20, No. 1-2 (1986), pp. 21-28.
(34) Kinoshita, K., "Particle Size Effects for Oxygen Reduction on Highly Dispersed Platinum in Acid Electrolytes", *J. Electrochem. Soc.*, Vol. 137, No. 3 (1990), pp. 845-848.
(35) Kabbabi, A. et al., "Particle Size Effect for Oxygen Reduction and Methanol Oxidation on Pt/C Inside a Proton Exchange Membrane", *J. Electroanal. Chem.*, Vol. 373, No. 1-2 (1994), pp. 251-254.
(36) Takasu, Y. et al., "Size Effects of Platinum Particles on the Electroreduction of Oxygen", *Electrochim. Acta*, Vol. 41, No. 16 (1996), pp. 2595-2600.
(37) Markovic, N. et al., "Kinetics of Oxygen Reduction on Pt (hkl) Electrodes: Implications for the Crystallite Size Effect with Supported Pt Electrocatalysts", *J. Electrochem. Soc.*, Vol. 144, No. 5 (1997), pp. 1591-1597.
(38) Mukerjee, S. and McBreen, J., "Effect of Particle Size on the Electrocatalysis by Carbon-supported Pt Electrocatalysts: An In Situ XAS Investigation", *J. Electroanal. Chem.*, Vol. 448, No. 2 (1998), pp. 163-171.
(39) Mayrhofer, K. J. J. et al., "The Impact of Geometric and Surface Electronic Properties of Pt-catalysts on the Particle Size Effect in Electrocatalysis.", *J. Phys. Chem. B*, Vol. 109, No. 30 (2005), pp. 14433-14440.
(40) Sarapuu, A. et al., "Electrochemical Reduction of Oxygen on Thin-film Pt Electrodes in Acid Solutions", *Electrochim. Acta*, Vol. 53, No. 20 (2008), pp. 5873-5880.
(41) Shao, M. et al., "Electrocatalysis on Platinum Nanoparticles: Particle Size Effect on Oxygen Reduction Reaction Activity", *Nano Lett.*, Vol. 11, No. 9 (2011), pp. 3714-3719.
(42) Tritsaris, G. A. et al., "Atomic-scale Modeling of Particle Size Effects for the Oxygen Reduction Reaction on Pt", *Catal. Lett.*, Vol. 141, No. 7 (2011), pp. 909-913.
(43) Sheng, W. et al., "Size Influence on the Oxygen Reduction Reaction Activity and Instability of Supported Pt Nanoparticles", *J. Electrochem. Soc.*, Vol. 159, No. 2 (2012), pp. B96-B103.
(44) Perez-Alonso, F. J. et al., "The Effect of Size on the Oxygen Electroreduction Activity of Mass-selected Platinum Nanoparticles", *Angew. Chem. Int. Ed.*, Vol. 51, No. 19 (2012), pp. 4641-4643.
(45) Papandrew, A. B. et al., "Oxygen Reduction Activity of Vapor-grown Platinum Nanotubes", *J. Electrochem. Soc.*, Vol. 160, No. 8 (2013), pp. F848-F852.
(46) Shinozaki, K. et al., "Suppression of Oxygen Reduction Reaction Activity on Pt-based Electrocatalysts from Ionomer Incorporation", *J. Power Sources*, Vol. 325 (2016), pp. 745-751.
(47) Subbaraman, R. et al., "Oxygen Reduction Reaction at Three-phase Interfaces", *ChemPhysChem*, Vol. 11, No. 13 (2010), pp. 2825-2833.
(48) Gómez-Marín, A. M. et al., "Spectroelectrochemical Studies of the Pt(111)/Nafion Interface Cast Electrode", *J. Phys. Chem. C*, Vol. 114, No. 47 (2010), pp. 20130-20140.
(49) Ahmed, M. et al., "Unprecedented Structural Sensitivity toward Average Terrace Width: Nafion Adsorption at Pt{*hkl*} Electrodes", *J. Phys. Chem. C*, Vol. 115, No. 34 (2011), pp. 17020-17027.
(50) Jinnai, H. et al., "Transmission Electron Microtomography and Polymer Nanostructures", *Macromolecules*, Vol. 43, No. 4 (2010), pp. 1675-1688.
(51) Shinozaki, K. et al., "Relative Humidity Dependence of Pt Utilization in Polymer Electrolyte Fuel Cell Electrodes: Effects of Electrode Thickness, Ionomer-to-carbon Ratio, Ionomer Equivalent Weight, and Carbon Support", *J. Electrochem. Soc.*, Vol. 158, No. 5 (2011), pp. B467-B475.
(52) Iden, H. and Ohma, A., "An In Situ Technique for Analyzing Ionomer Coverage in Catalyst Layers", *J. Electroanal. Chem.*, Vol. 693 (2013), pp. 34-41.
(53) Ikeda, K. et al., "Analysis of the Ionomer Coverage of Pt Surface in PEMFC", *ECS Trans.*, Vol. 33, No. 1 (2010), pp. 1189-1197.
(54) Lopez-Haro, M. et al., "Three-dimensional Analysis of Nafion Layers in Fuel Cell Electrodes", *Nature Commun.*, Vol. 5, No. 5229 (2014).

Figs. 14 and 15
Reprinted from J. Power Sources, Vol. 325 (2016), pp. 745-751, Shinozaki, K. et al., Suppression of Oxygen Reduction Reaction Activity on Pt-based Electrocatalysts from Ionomer Incorporation, © 2016 Elsevier, with permission from Elsevier.

Kazuma Shinozaki
Research Field:
- Proton Exchange Membrane Fuel Cell

Academic Degree: Ph.D.
Academic Society:
- The Electrochemical Society of Japan

Yu Morimoto
Research Fields:
- Electrochemical Devices
- Fuel Cells

Academic Degree: Ph.D
Academic Societies:
- The Electrochemical Society
- The Electrochemical Society of Japan

Jason W. Zack*
Research Field:
- RDE FC Catalysts Evaluation

Svitlana Pylypenko**
Research Fields:
- Surface and Interface Analysis
- Multiscale and In Situ/Operando Characterization
- Fuel Cells
- Batteries and Electrolysis

Academic Degree: Ph.D.
Academic Societies:
- The Electrochemical Society
- American Vacuum Society
- The American Chemical Society

Ryan M. Richards*, **
Research Fields:
- Nanoscience
- Catalysis

Academic Degree: Ph.D.
Academic Societies:
- The American Chemical Society
- North American Catalysis Society

Award:
- Fellow of the American Chemical Society, 2014

Bryan S. Pivovar*
Research Fields:
- Proton Exchange Membrane Fuel Cell
- PEM Electrolysis
- Alkaline Membranes
- Electrocatalysis

Academic Degree: Ph.D.
Academic Societies:
- The Electrochemical Society
- The American Chemical Society
- American Institute of Chemical Engineers

Awards:
- Charles W. Tobias Young Investigator Award, The Electrochemical Society, 2012
- Hydrogen and Fuel Cells Program Award, DOE, 2016, 2018

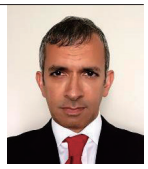

Shyam S. Kocha***
Research Fields:
- Proton Exchange Membrane Fuel Cell
- Electrolysis

Academic Degree: Ph.D.
Academic Society:
- The Electrochemical Society

*National Renewable Energy Laboratory
**Colorado School of Mines
***Resigned from National Renewable Energy Laboratory